Supplementary information:

Interfacially-localized high-concentration electrolytes for high-performance rechargeable aqueous lithium-ion batteries

Guohong Shen[1], Shinji Kondou[2], Gakuto Wada[1], Hiroki Nakagaki[1], Masayoshi Watanabe[3], Kaoru Dokko[1,3], Kazuhide Ueno[1,3,*]

[1] *Department of Chemistry and Biotechnology, Yokohama National University, 79-5 Tokiwadai, Hodogaya-ku, Yokohama 240-8501, Japan*

[2] *Department of Materials Engineering Science, Graduate School of Engineering Science, Osaka University, 1-3 Machikaneyama, Toyonaka, Osaka 560-8531, Japan*

[3] *Institute of Advanced Sciences, Yokohama National University, 79-5 Tokiwadai, Hodogaya-ku, Yokohama 240-8501, Japan*

E-mail: ueno-kazuhide-rc@ynu.ac.jp

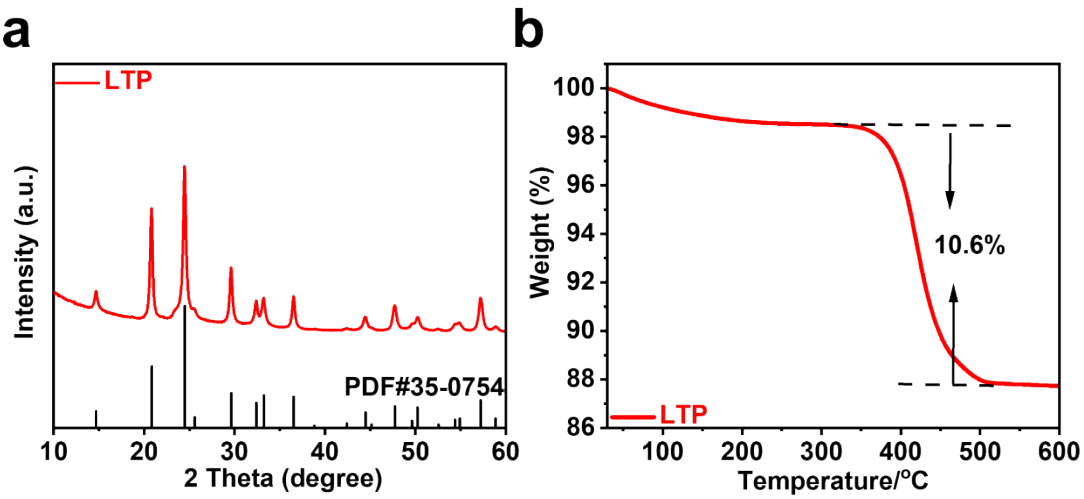

Figure S1. (a) XRD pattern of prepared LTP at a scan speed of 5° min^{-1} and (b) TGA of prepared LTP under a N_2 atmosphere, and heating rate of 5 °C min^{-1}.

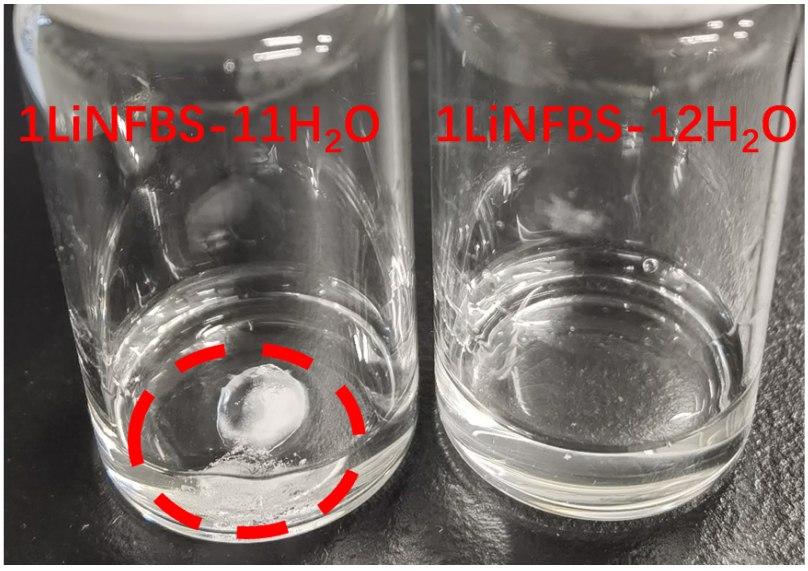

Figure S2. Digital photographs of the LiNFBS-11H_2O and LiNFBS-12H_2O electrolytes (molar ratio). The red-dotted circular area represent gel-like substance.

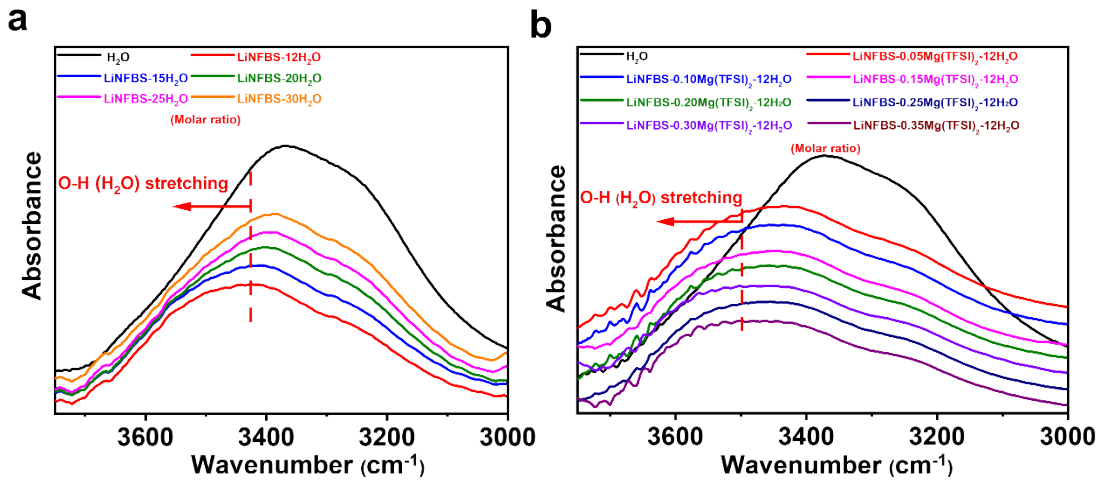

Figure S3. FTIR of electrolytes containing (a) LiNFBS-xH$_2$O (x = 12-30, molar ratio) and (b) LiNFBS-yMg(TFSI)$_2$-12H$_2$O (y= 0.05-0.35, molar ratio).

Table S1. Physical and chemical properties of electrolytes containing LiNFBS-(12-25) H$_2$O (Molar ratio).

Electrolytes (Molar ratio, 30 °C)	η (mPa s)	σ (mS cm^{-1})	Molar Concentration (mol L^{-1})	ρ (g cm^{-3})
LiNFBS:12 H$_2$O	19.2	58.7	2.70 M	1.41
LiNFBS:15 H$_2$O	14.2	62.3	2.36 M	1.36
LiNFBS:20 H$_2$O	8.7	63.9	1.95 M	1.30
LiNFBS:25 H$_2$O	5.4	56.4	1.66 M	1.26

Table S2. Physical and chemical properties of electrolytes containing LiNFBS-(0.05-0.35Mg(TFSI)$_2$)-12H$_2$O (Molar ratio).

Electrolytes (Molar ratio, 30 °C)	η (mPa s)	σ (mS cm^{-1})	Molar Concentration (mol L^{-1})	ρ (g cm^{-3})
LiNFBS:12H$_2$O	19.2	58.7	2.70 M	1.41
LiNFBS:0.05Mg(TFSI)$_2$:12H$_2$O	18.5	55.4	2.60 M:0.13 M	1.43
LiNFBS:0.10Mg(TFSI)$_2$:12H$_2$O	17.9	50.5	2.50 M:0.25 M	1.45
LiNFBS:0.15Mg(TFSI)$_2$:12H$_2$O	17.7	48.0	2.42 M:0.36 M	1.48
LiNFBS:0.20Mg(TFSI)$_2$:12H$_2$O	17.8	47.6	2.34 M:0.46 M	1.49
LiNFBS:0.25Mg(TFSI)$_2$:12H$_2$O	17.9	40.7	2.26 M:0.56 M	1.51
LiNFBS:0.30Mg(TFSI)$_2$:12H$_2$O	18.6	37.4	2.19 M:0.66 M	1.53
LiNFBS:0.35Mg(TFSI)$_2$:12H$_2$O	19.2	34.0	2.13 M:0.74M	1.54

Table S3. Surface tension of solution containing 0.74 M $Mg(TFSI)_2$.

Sample (Molar concentration)	Surface tension γ (mN m^{-1})
0.74 M $Mg(TFSI)_2$	45.3

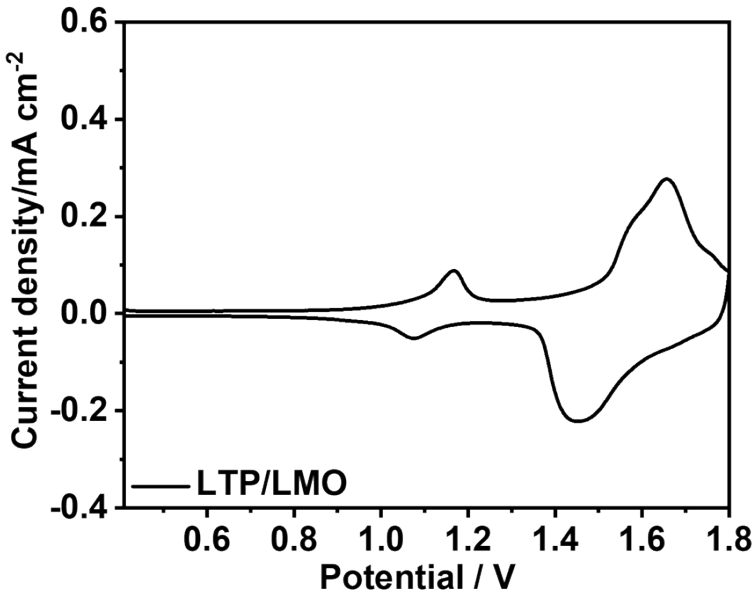

Figure S4. Cyclic voltammogram (CV) of LTP/LMO full cells containing LiNFBS-0.35$Mg(TFSI)_2$-12H_2O at a scan rate of 0.1 mV s^{-1} .

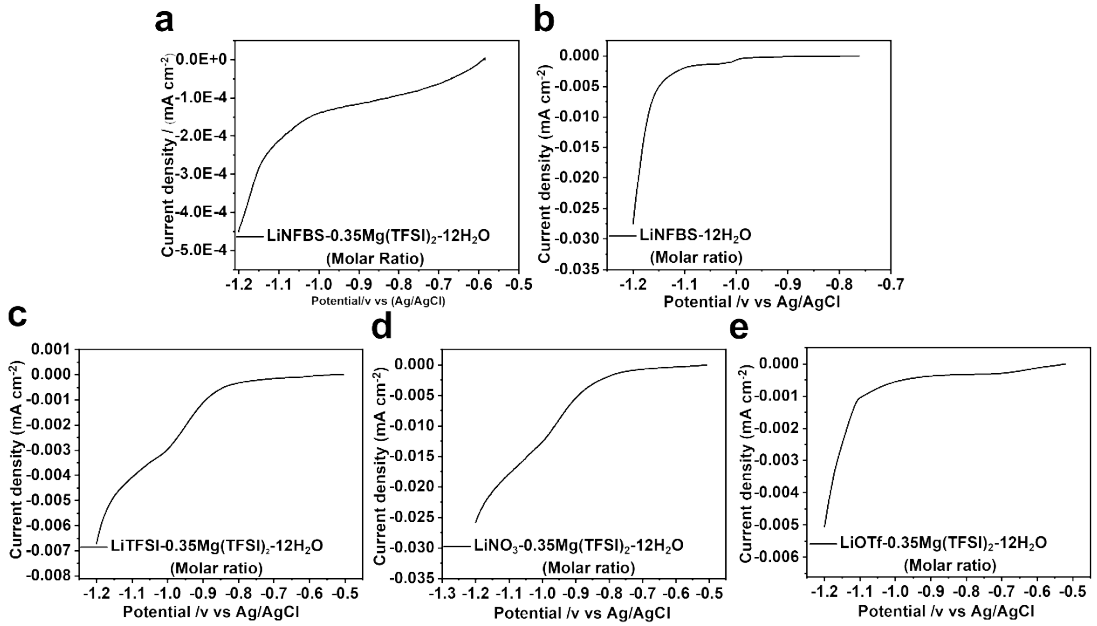

Figure S5. LSV curves of Al working electrode from OCV to –1.2 V vs. Ag/AgCl using different electrolytes containing: (a) LiNFBS- 0.35Mg(TFSI)$_2$-12H$_2$O, (b) LiNFBS-12H$_2$O, (c) LiTFSI- 0.35Mg(TFSI)$_2$-12 H$_2$O, (d) LiNO$_3$- 0.35Mg(TFSI)$_2$-12H$_2$O, and (e) LiOTf- 0.35Mg(TFSI)$_2$-12H$_2$O.

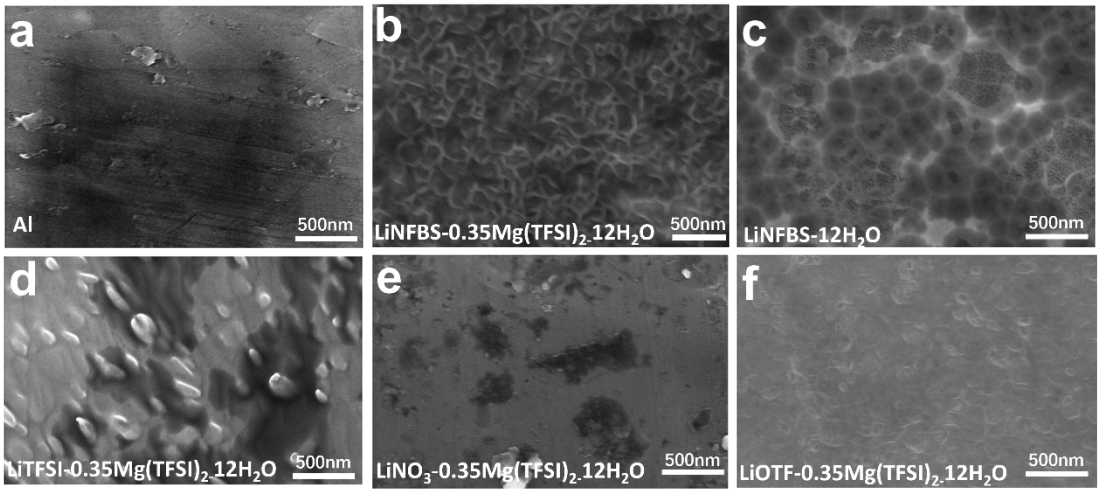

Figure S6. Magnification of SEM images of Al electrode surface after potentiostatic polarization for 20 h at −1.2 V vs. Ag/AgCl using different electrolytes: (a) pristine Al foil; (b) LiNFBS-0.35 Mg(TFSI)$_2$-12H$_2$O; (c) LiNFBS-12H$_2$O; (d) LiTFSI-0.35Mg(TFSI)$_2$-12H$_2$O; (e) LiNO$_3$-0.35Mg(TFSI)$_2$-12H$_2$O; (f) LiOTf-0.35Mg(TFSI)$_2$-12H$_2$O.

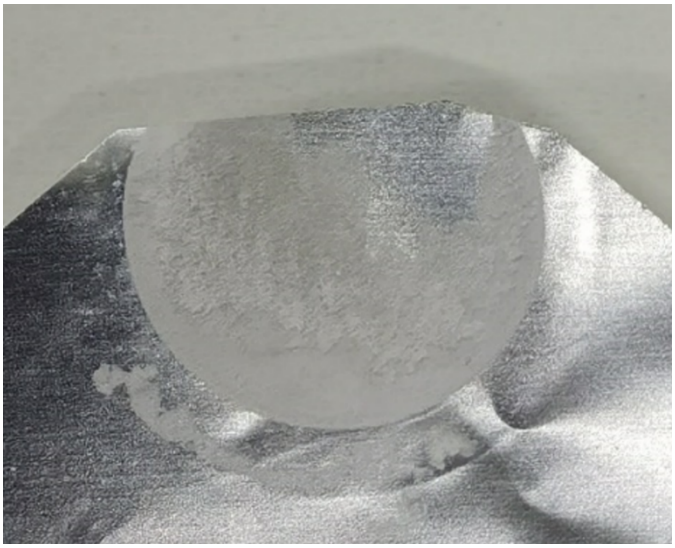

Figure S7. Digital photographs of Al working electrode at −1.2 V vs. Ag/AgCl for 20 h using the electrolytes composed of $LiNO_3$-0.35$Mg(TFSI)_2$-12H_2O (Molar ratio).

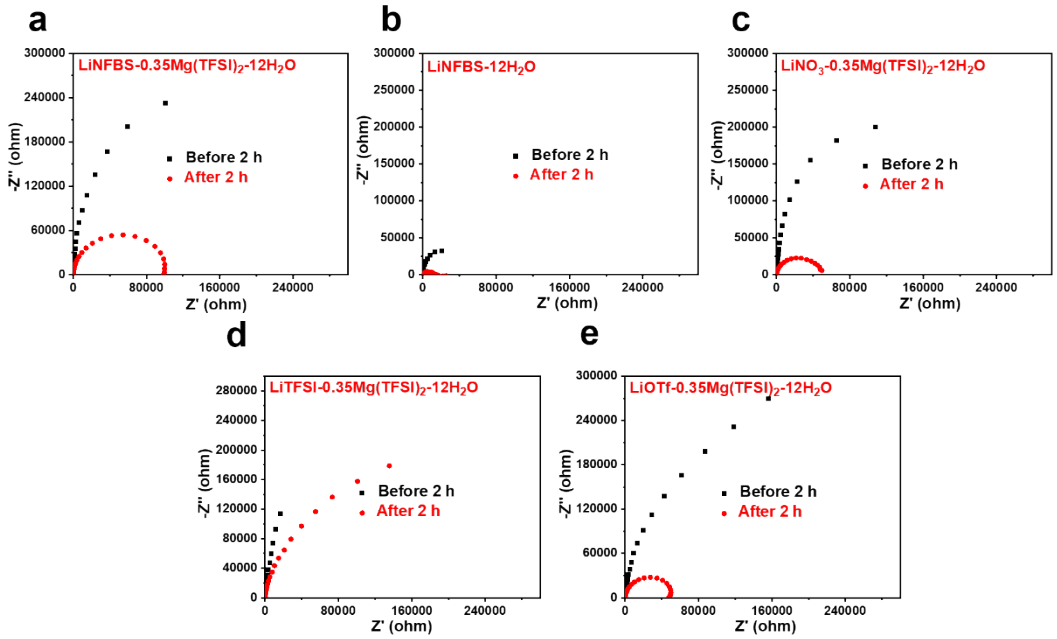

Figure S8. Electrochemical Impedance Spectroscopy (EIS) of Al electrode before and after potentiostatic polarization for 2 h at −1.2 V vs. Ag/AgCl using different electrolytes: (a) LiNFBS-0.35 $Mg(TFSI)_2$-12H_2O; (b) LiNFBS-12H_2O; (c) LiTFSI-0.35$Mg(TFSI)_2$-12H_2O; (d) $LiNO_3$-0.35$Mg(TFSI)_2$-12H_2O; (e) LiOTf-0.35$Mg(TFSI)_2$-12H_2O.

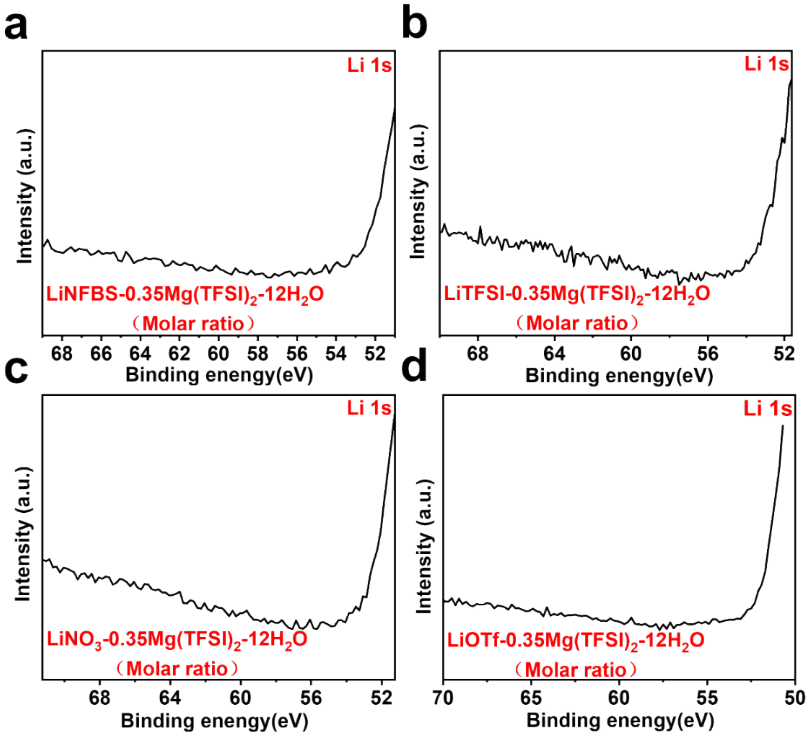

Figure S9. Li 1s XPS Spectra of Al working electrode after chronoamperometry (CA) for 20 h at -1.2 V vs Ag/AgCl using electrolytes containing: (a) LiNFBS-0.35Mg(TFSI)$_2$-12H$_2$O, (b) LiTFSI-0.35Mg(TFSI)$_2$-12H$_2$O, (c) LiNO$_3$-0.35Mg(TFSI)$_2$-12H$_2$O, and (d) LiOTf-0.35Mg(TFSI)$_2$-12H$_2$O.

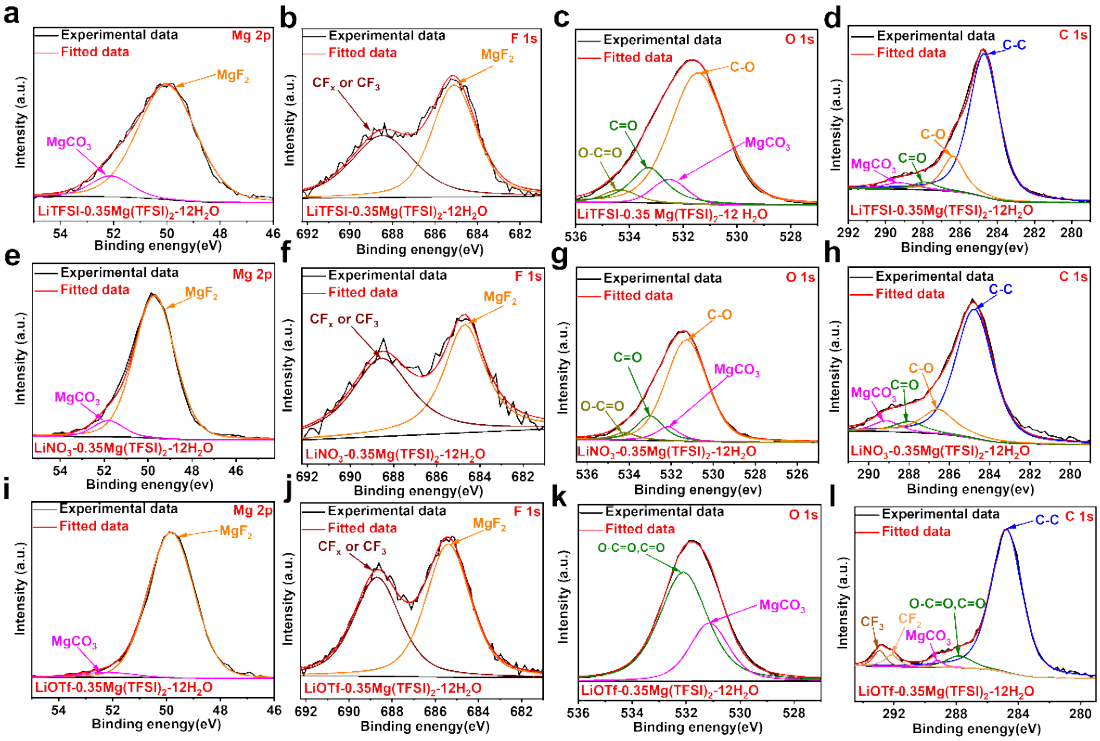

Figure S10. XPS Spectra of Al electrode after polarization for 20 h at −1.2 V vs Ag/AgCl and LiNFBS-12H$_2$O: (a) Mg 2p, (b) F 1s, (c) O 1s, (d) C 1s spectra in LiTFSI-

0.35Mg(TFSI)$_2$-12H$_2$O and (e) Li 1s, (f) F 1s, (g) O 1s, (h) C 1s in LiNO$_3$-0.35Mg(TFSI)$_2$-12H$_2$O, and (i) Li 1s, (j) F 1s, (k) O 1s, (l) C 1s in LiOTf-0.35Mg(TFSI)$_2$-12H$_2$O.

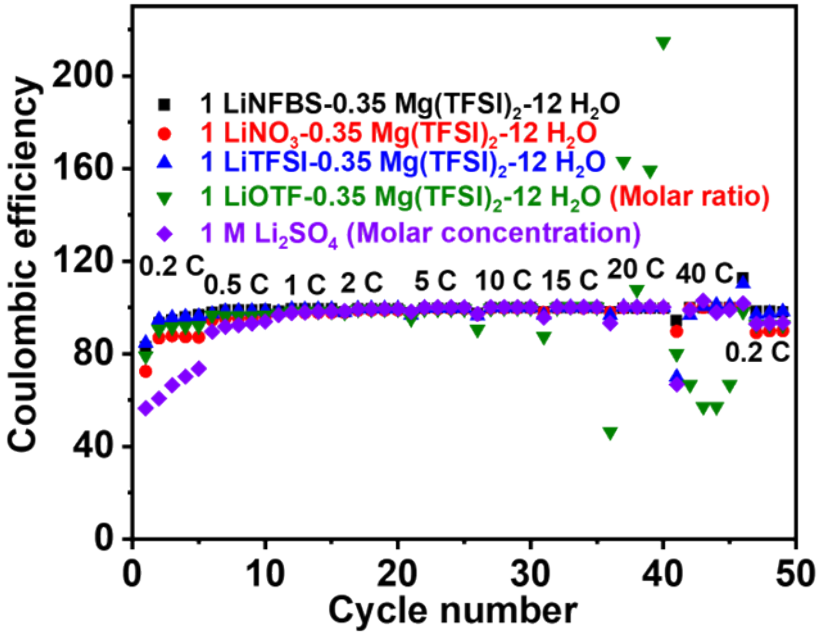

Figure S11. Coulombic efficiency of LTP/LMO full cells using electrolytes LiNFBS-0.35Mg(TFSI)$_2$-12H$_2$O, LiNO$_3$-0.35Mg(TFSI)$_2$-12H$_2$O, LiTFSI-0.35Mg(TFSI)$_2$-12H$_2$O, LiOTf-0.35Mg(TFSI)$_2$-12H$_2$O, and 1 M Li$_2$SO$_4$ at different current density from 0.2 to 40 C.

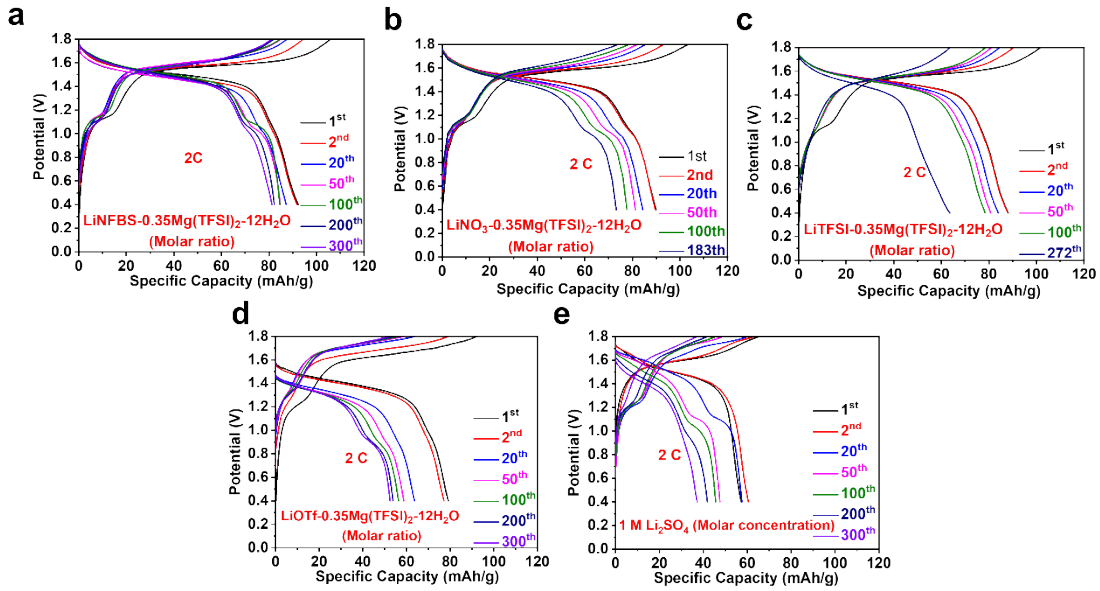

Figure S12. Charge-discharge curves of LTP/LMO full batteries using electrolytes composed of: (a) LiNFBS-0.35Mg(TFSI)$_2$-12H$_2$O, (b) LiNO$_3$-0.35Mg(TFSI)$_2$-12H$_2$O, (c) LiTFSI-0.35Mg(TFSI)$_2$-12H$_2$O, (d) LiOTf-0.35Mg(TFSI)$_2$-12H$_2$O, and (e) 1 M

Li_2SO_4 at a current rate of 2 C.

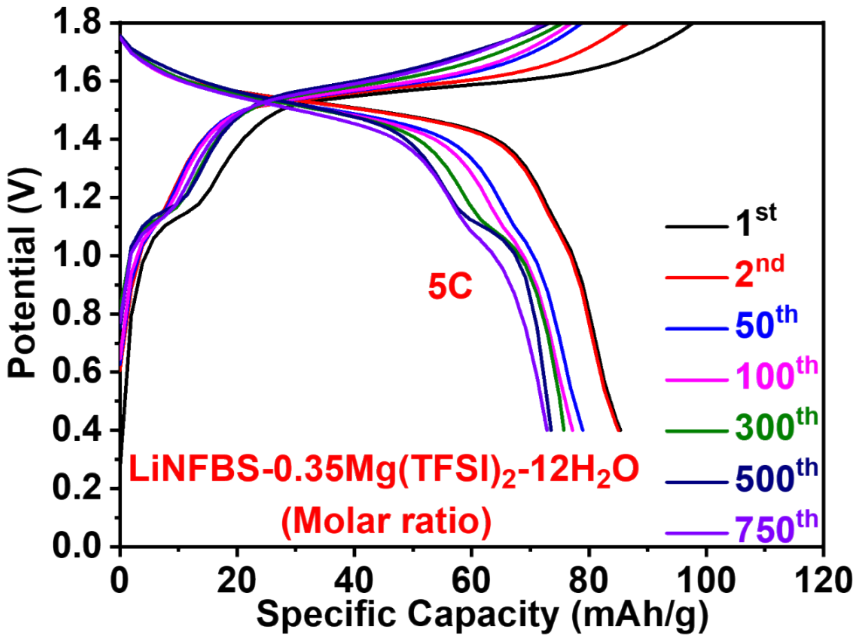

Figure S13. Charge-discharge curves of LTP/LMO full cell using LiNFBS-0.35Mg(TFSI)$_2$-12H$_2$O at a current rate of 5 C.

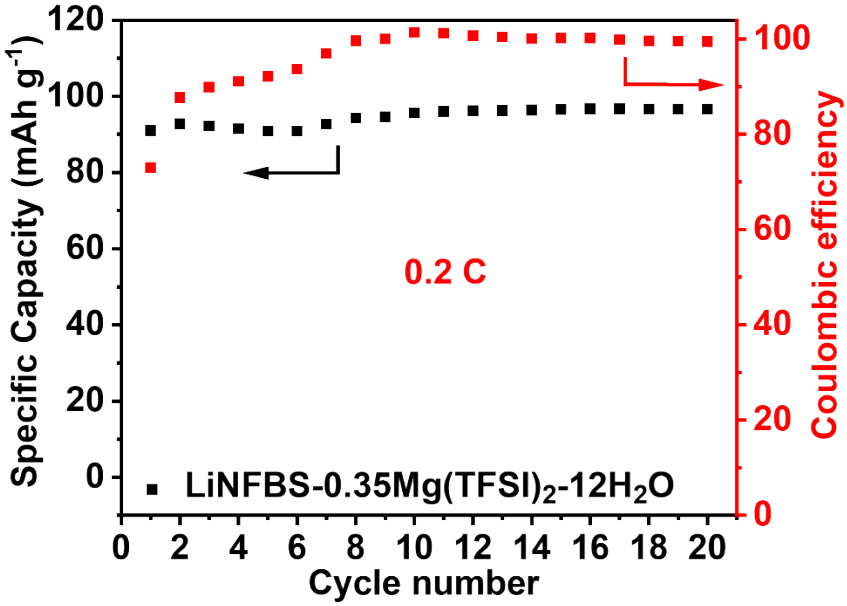

Figure S14. Long cycling performance of the cell containing LiNFBS-0.35Mg(TFSI)$_2$-12H$_2$O at current density of 0.2 C.

Table S4. Performance Comparison of Different Electrolyte Systems.

Electrolytes/Electrode	ESW	Current Density	Capacity Retention	References
25 mol L^{-1} CH_3COONH_4+5 mol L^{-1} CH_3COONa (MnO_2/CNTs||NTP/C)	3.9 V	0.1 A g^{-1}	70 % (500 cycles)	Ref.65
BSiS-$DOL_{0.5}$ (LMO||LTO)	4.7 V	5 C	50% (2000 cycles)	Ref.66
1.85 m LiTFSI-H_2O-IDE (LMO||LTO)	4.3 V	2 C	72% (450 cycles)	Ref.67
LiNFBS:0.35Mg(TFSI)$_2$:12H_2O (LMO||LTP)	**3.3 V**	**5 C**	86 % (750 cycles)	**This work**